Acta Pharmaceutica Sinica B 2021;11(11):3622–3635

Chinese Pharmaceutical Association
Institute of Materia Medica, Chinese Academy of Medical Sciences

Acta Pharmaceutica Sinica B

www.elsevier.com/locate/apsb
www.sciencedirect.com

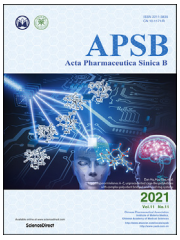

ORIGINAL ARTICLE

Genetically-engineered "all-in-one" vaccine platform for cancer immunotherapy

Aihua Wu[a,b], Yingzhi Chen[a], Hairui Wang[a,b], Ya Chang[a], Meng Zhang[a], Pengfei Zhao[a], Yisi Tang[a,b], Qin Xu[b,*], Zhuangzhi Zhu[c], Yang Cao[b], Yongzhuo Huang[a,d,e,f,*]

[a]*State Key Laboratory of Drug Research, Shanghai Institute of Materia Medica, Chinese Academy of Sciences, Shanghai 201203, China*
[b]*Artemisinin Research Center, the First Affiliated Hospital, Guangzhou University of Chinese Medicine, Guangzhou 510450, China*
[c]*National Pharmaceutical Engineering Research Center, China State Institute of Pharmaceutical Industry, Shanghai 201203, China*
[d]*Zhongshan Institute for Drug Discovery, Institutes of Drug Discovery and Development, Chinese Academy of Sciences, Zhongshan 528437, China*
[e]*University of Chinese Academy of Sciences, Beijing 100049, China*
[f]*NMPA Key Laboratory for Quality Research and Evaluation of Pharmaceutical Excipients, Shanghai 201203, China*

Received 20 March 2021; received in revised form 8 May 2021; accepted 11 May 2021

KEY WORDS

Trichosanthin;
Legumain;
TRP2;
Transcutaneous immunization;
Adjuvant;
Cancer vaccine;
Protein engineering

Abstract An essential step for cancer vaccination is to break the immunosuppression and elicit a tumor-specific immunity. A major hurdle against cancer therapeutic vaccination is the insufficient immune stimulation of the cancer vaccines and lack of a safe and efficient adjuvant for human use. We discovered a novel cancer immunostimulant, trichosanthin (TCS), that is a clinically used protein drug in China, and developed a well-adaptable protein-engineering method for making recombinant protein vaccines by fusion of an antigenic peptide, TCS, and a cell-penetrating peptide (CPP), termed an "all-in-one" vaccine, for transcutaneous cancer immunization. The TCS adjuvant effect on antigen presentation was investigated and the antitumor immunity of the vaccines was investigated using the different tumor models. The vaccines were prepared *via* a facile recombinant method. The vaccines induced the maturation of DCs that subsequently primed $CD8^+$ T cells. The TCS-based immunostimulation was associated with the STING pathway. The general applicability of this genetic engineering strategy was demonstrated with various tumor antigens (*i.e.*, legumain and TRP2 antigenic peptides) and tumor models

*Corresponding authors. Tel./fax: +86 21 20231981 (Yongzhuo Huang).
E-mail addresses: xuqin@gzucm.edu.cn (Qin Xu), yzhuang@simm.ac.cn (Yongzhuo Huang).

Peer review under responsibility of Chinese Pharmaceutical Association and Institute of Materia Medica, Chinese Academy of Medical Sciences.

https://doi.org/10.1016/j.apsb.2021.06.001

(*i.e.*, colon tumor and melanoma). These findings represent a useful protocol for developing cancer vaccines at low cost and time-saving, and demonstrates the adjuvant application of TCS—an old drug for a new application.

1. Introduction

Cancer immunotherapy has been booming in recent years. The primary effect of cancer immunotherapy is to activate the suppressed immune system and reinstall the powerful immunity to annihilate the tumors. Therapeutic cancer vaccination has been a long-sought goal in the field of immunotherapy. Despite the enthusiastic input to cancer vaccine development, the clinical success of cancer therapeutic vaccines is limited, because of their suboptimal immunogenicity[1]. As a result, cancer therapeutic vaccines are typically the products of dendritic cells (DC) that are pre-challenged by a tumor antigen before infusion to the patients. It is well accepted that the better adjuvants than the currently licensed are needed, which should be potent enough to break the immunotolerance and elicit the desired immunity[2]. Although many adjuvants have been explored for cancer immunotherapy, most of them are poorly druggable due to lack of biosafety scrutiny. So far, only five adjuvants have been approved by U.S. Food and Drug Administration (FDA) for human use.

Trichosanthin (TCS) is a type I ribosome-inactivating protein, derived from the root of *Trichosanthes kirilowii Maxim*. that has been used as a Chinese herb *Tian Hua Fen* for over a thousand years. Trichosanthin Injection is an approved gynecological drug in China to treat hydatidiform mole, extrauterine pregnancy, stillbirth, as well as abortion. TCS also bears the potent antitumor activities[3]. The primary anticancer mechanism of TCS is its ribosome-inactivating effect. We have demonstrated its anticancer potential in various tumor models including fibrosarcoma, glioma, and drug-resistant lung tumor[4−6]. However, the native TCS is hardly clinically serviceable as an i.v. administered cancer drug candidate because of its short half-life and poor tumor distribution and cell penetration ability. We previously found that its interaction with effector T cells also played a role in its antitumor effect[5], but its feasibility in cancer immunization has not been investigated yet.

We proposed a novel perception of TCS-assisted cancer vaccination and developed a general method for preparing a multifunctional genetically-engineered vaccine, in which a cell-penetrating peptide and tumor-specific antigenic peptide were introduced to each terminus of TCS, thus constructing an “all-in-one” including all the functional components (*i.e.*, tumor antigen, adjuvant, delivery-enhanced motif) of a vaccine.

Legumain, known as asparagine endopeptidase, is a tumor-associated protease in solid tumors and overexpressed in endothelial cells of neovasculature and tumor-associated macrophages (TAMs)[7,8]. Legumain is closely related to the tumoregenesis and progression[9], and can serve as a potential indicator for the transition from inflammation to cancer[10], a prognostic and metastatic biomarker[11], as well as a drug target[12]. Its therapeutic value as a tumor antigen for vaccination targeting TAMs has been revealed[13,14].

We designed an “all-in-one” vaccine by recombinant fusion of three major active components—a cell-penetrating sequence (low-molecular-weight protamine, LMWP), the TCS adjuvant domain, and the antigenic legumain peptide ($LGMN_{108-120}$)[15]—for treating the highly malignant colon cancer. LMWP is a potent cell-penetrating sequence identified from a clinically used drug protamine, and its safety has been demonstrated in dogs[16,17]. Importantly, the ability of LMWP-assisted cutaneous delivery has been demonstrated in our previous work and other groups’ works[17−19]. Therefore, the local administration could take advantage of the LMWP-assisted cutaneous delivery; LMWP could also promote the cellular uptake of the vaccine into the epidermis antigen-presenting cells.

Furthermore, another protein vaccine was designed by the same method in order to test the universality of this TCS-enhanced vaccination strategy. We used a tyrosinase-related protein-2 (TRP2) peptide as antigen, and prepared a cell-penetrating LWMP-TCS-TRP2 fusion protein vaccine.

2. Materials and methods

2.1. Reagents

The original recombinant TCS plasmid was kindly provided by Prof. Pang-Chui Shaw, The Chinese University of Hong Kong. *Escherichia coli* (*E. coli*) strain BL21 (DE3) was preserved by our laboratory. And the IMPACT (Intein-mediated purification with affinity chitin-binding tag) system, including the expressing vector pTXB1 and chitin resin, was obtained from New England Biolabs (UK). Lysogeny Broth (LB) medium was purchased from Oxoid (UK). The legumain antigenic peptide (sequence: EDVTPENFLAVLR) and TRP2 antigenic peptide (sequence: SVYDFFVWL) were synthesized by Nanjing Peptide Biotechnology Co., Ltd. (Nanjing, China). Bovine serum albumin (BSA) was obtained from RBC Life Sciences (USA). Succinimidyl 4-(*N*-maleimidomethyl) cyclohexane-1-carboxylate (SMCC) was obtained from ProteoChem (Loves Park, USA). Thiolated LMWP (sequence: CVSRRRRRRGGRRRR) were provided by Bankpeptide Co., Ltd., China. Protein markers and isopropyl β-D-1-thiogalactopyranoside (IPTG) were from Thermo Scientific (USA). Bradford and BCA Microplate Protein Assay Kits were obtained from Beyotime Institute of Biotechnology (Haimen, China). Cocktail protease inhibitor, 3-(4,5-dimethylthiazol-2-yr)-2,5-diphenyltetrazolium bromide (MTT), and lipopolysaccharide (LPS) was purchased from Sigma−Aldrich (USA). Fetal bovine serums (FBS), 1640 cell culture medium, Dulbecco’s modified Eagle’s medium (DMEM) cell culture medium and 0.25% trypsin−EDTA were purchased from Gibco® Thermo Fisher Scientific (USA). The antibiotics were obtained from Amresco (USA). L-Cysteine was obtained from J&K Scientific Ltd. (Shanghai, China). Rhodamine B was obtained from

Meilun Biotechnology Co., Ltd. (Dalian, China). Murine GM-CSF and murine IL-4 purchased from Novus Biologicals (R&D System, USA). Anti-MHCI, anti-MHCII, anti-mannose receptor (CD206), anti-legumain, anti-TNF-α, anti-TGF-β, anti-IRF3, and anti-STING (anti-TMEM173) antibodies were from Abcam (UK). Anti-CD8 alpha and anti-Foxp3 antibodies were obtained from Novus Biologicals (R&D System, USA). Anti-CD11c-PerCP-Cy5.5, anti-CD80-FITC, anti-CD86-PE, anti-CD3 alpha-PerCP, anti-CD4-FITC, and anti-CD8-PE antibodies were purchased from BD Biosciences (USA). Murine TNF-α, TGF-β, IL-2, and IL-10 ELISA Kit were purchased from Shanghai Dakewe Biotech Co., Ltd. (Shanghai, China). Mouse IFN-γ ELISA Kit was purchased from R&D Systems (USA). All other reagents were of analytical grade from Sinapharm Chemical Reagent Co., Ltd. (Shanghai, China).

2.2. Cell lines and mice

Murine colon cancer cell line CT26, murine B16-F10 melanoma cells, and dendritic cell line DC2.4 were obtained from Shanghai Cell Bank of Chinese Academy of Sciences (Shanghai, China). The cells were cultured at 37 °C under 5% CO_2 in complete medium consisting of RPMI-1640 medium or DMEM, supplemented with 10% (*v*/*v*) heat-inactivated fetal bovine serum, penicillin (100 μg/mL), and streptomycin (100 μg/mL). Female BALB/c mice (6−8 weeks) and female C57BL/6 mice (6−8 weeks) were obtained from Shanghai Laboratory Animal Center (SLAC) Co., Ltd. (Shanghai, China), and housed at the SPF care facility with sterilized food pellets and distilled water under a 12-h light/dark cycle. The mice were allowed to adapt to their environment for one week before the experiments. All the animal experimental procedures were approved by Institutional Animal Care and Use Committee (IACUC), Shanghai Institute of Materia Medica (SIMM), Chinese Academy of Sciences. (Note: SIMM is an institution with AAALAC International accreditation.)

2.3. Protein construction

The sequence of low molecular weight protamine (LMWP, VSRRRRRRGGRRRR) was added to the N-terminus of TCS and the legumain antigenic sequence (EDVTPENFLAVLR) to the C-terminus of TCS by polymerase chain reaction (PCR) to prepare the recombinant gene encoding the fusion protein of LMWP-TCS-legumain (rLTL). The rLTL sequence was subcloned to an intein-mediated protein expressing vector pMXB10 at Ndel and Xhol site to prepare the pLTL plasmid, using a method modified from our previous report[40]. The control fusion proteins, *i.e.*, TCS-legumain (rTCS-leg) and rTCS, were also prepared. Similarly, the TCS-TRP2 (rTCS-TRP2) and LMWP-TCS-TRP2 (rLTT) fusion proteins were prepared, respectively. The TRP2 sequence (SVYDFFVWL) was added to the C-terminus of TCS and the LMWP sequence to the N-terminus.

2.4. Protein expression

The recombinant plasmids were transformed into *E. coli* BL21 (DE3). Bacteria cultures were incubated at 37 °C in the LB medium containing 100 μg/mL ampicillin sodium until the optical density at 600 nm reached 0.5−0.8. Then the target protein expression was induced at 25 °C overnight by the addition of IPTG at the final concentration of 0.3 mmol/L.

2.5. Protein purification

The rTCS, rTCS-leg, rLTL, rTCS-TRP2, and rLTT were expressed and purified using the IMPACT system (NEB) according to the manufacturer's instructions with minor modifications. Briefly, the induced bacterial culture was harvested by centrifugation at 8900×*g* (Sorvall ST16, Thermo Scientific, USA) for 3 min and the bacteria were suspended in the column buffer (20 mmol/L HEPES-Na, 500 mmol/L NaCl, 1 mmol/L EDTA, pH 8.5). The suspensions were sonicated (400 W, 30 min) and centrifuged at 16,000×*g* at 4 °C for 30 min. The supernatant containing the soluble target proteins was loaded on the pre-equilibrated chitin gravity column at a speed of approximately 1 mL/min. The columns were flushed sequentially with 20-column volumes of buffer to remove the unbound proteins, and 3-bed volumes of cleavage buffer (the column buffer containing 50 mmol/L cysteine) to perform the on-column cleavage. The columns were then incubated with the cleavage buffer at 4 °C for 16 h, followed by elution and collection of the target proteins.

The proteins were purified using FPLC (AKTApurifier 10, GE Healthcare, USA). After purification by a desalting column (GE Healthcare, USA) with PBS buffer (pH 7.2), small molecules were removed. The expression of the soluble protein was examined by BCA microplate protein assay kit. The final products were characterized using SDS-PAGE electrophoresis, MALDI-TOF-MS (MALDI TOF/TOF 5800 analyzer, AB Sciex, Framingham, MA, USA), and size exclusion chromatography (Superdex 75, GE healthcare). The LPS content in the purified recombinant proteins was monitored by an Endotoxin Assay Kit (Xiamen Bioendo Technology Co., Ltd., China) according to the manufacturer's instructions. The proteins used *in vivo* experiment were all under the endotoxin limit in FDA guideline for non-intrathecal drug products.

2.6. Preparation of the LMWP-BSA-leg

BSA was activated by SMCC. In brief, SMCC (20 mg/mL in DMSO) was added dropwise to the BSA solution (20 mg/mL in PBS, pH 7.2) at a molar ratio of 2:1 and reacted under magnetic stirring for 1 h. The activated BSA was purified using FPLC (ÄKTApurifier 10, GE Healthcare, USA) equipped with a desalting column (GE Healthcare, USA) and subsequently reacted with the thiolated LMWP (sequence: CVSRRRRRRGGRRRR) and legumain antigenic peptide (sequence: CEDVTPENFLAVLR) in PBS (pH 7.2) for 12 h at 4 °C. The final product was purified by using a desalting column. The concentration of the purified LMWP-BSA-leg was determined by a standard BCA method.

2.7. In vitro cytotoxicity assay

DC2.4 cells were used to investigate the cytotoxicity of the protein vaccines using a standard MTT assay. The cells were seeded in a 96-well plate at a density of 5000 cells per well. After exposure to the proteins for 48 h, the cell viability was measured. All cytotoxicity assay experiments were performed in quintuplicate and the cell viability was calculated using Eq. (1).

$$\text{Cell viability}\,(\%) = (A_{\text{test}} - A_{\text{blank}}) / (A_{\text{control}} - A_{\text{blank}}) \times 100 \quad (1)$$

2.8. Cellular uptake

The DC2.4 cells were seeded in the 12-well plates at a density of 1×10^5 cell/well and cultured for 24 h. The proteins were labeled by rhodamine B isothiocyanate. The DC2.4 cells were incubated with the proteins for 4 h at 37 °C. Subsequently, the cells rinsed with cold PBS, fixed with 4% paraformaldehyde and stained with DAPI (4′,6-diamidino-2-phenylindole). Fluorescent images were observed with a fluorescence microscope (Zeiss, Germany). In addition, the cellular uptake efficiency was determined by using a flow cytometer (BD Pharmingen, USA).

2.9. Generation of mouse BMDCs

BMDCs were prepared as a previous report[28] with minor modifications. Briefly, the femurs and tibiae from the 6−8 weeks BALB/c mice or C57BL/6 mice were used to collect the bone marrow cells using PBS buffer flushing, and the RBC lysis buffer (Sigma−Aldrich, USA) was added to deplete the erythrocytes. The collected precursors were cultured in DMEM complete medium containing 20 ng/mL of recombinant murine GM-CSF and 10 ng/mL of IL-4 for 3 days and the nonadherent cells were discarded. Following additional culture for 4 days, the loosely adherent BMDCs were harvested and used as immature DCs (iDCs). The purity of iDCs was measured to be >85% by detecting the fluorescent-labeled anti-CD11c monoclonal antibody staining using flow cytometry.

2.10. Isolation of murine T cells

T cells were isolated from the spleens of the BALB/c mice or C57BL/6 mice and purified using lymphocyte separation medium. Briefly, the cell suspension was prepared by cutting the spleen into small pieces that were then extruded through a 70-μm cell strainer (Falcon, BD, CA, USA) using a syringe plunger. After centrifugation, the lymphocytes were collected and suspended in the complete T cell medium.

2.11. Effects of the vaccines on BMDC maturation and antigen presentation assay

The BMDCs were prepared as described above. The BMDCs were seeded at a density of 1×10^5 cells per well in a 12-well plate and incubated with 670 ng/mL LPS (positive control) or different vaccine formulations for 18 h. The cells were subsequently labeled with PerCP-Cy5.5-labeled anti-mouse CD11c, FITC-labeled anti-mouse CD80, and PE-labeled anti-mouse CD86 monoclonal antibodies for 30 min at 4 °C. After wash, the cells were subjected to flow cytometric assay. For the antigen presentation assay, the BMDCs treated with various vaccines for 18 h were stained with MHC I and MHC II monoclonal antibodies and then subjected to flow cytometry.

2.12. Effects of proteins on T-cell proliferation

The responder T cells isolated from the spleens of the BALB/c mice C57BL/6 mice were cocultured with the BMDCs that were pretreated with different vaccines for 18 h at a ratio of 5:1 (T/DC) for 3 days in the complete RPMI-1640 medium. The IFN-γ level in the supernatants was measured using an ELISA kit according to the manufacturer's instructions.

2.13. In vitro cytotoxic T cell killing assay

BMDCs were prepared as described above. The BMDCs were seeded at a density of 2×10^5 cells per well in a 6-well plate and incubated with 670 ng/mL LPS (positive control), rLTT, or varying vaccine formulations for 18 h. These pretreated BMDCs were subsequently co-cultured with the responder T cells isolated from the spleens of the C57BL/6 mice at a ratio of 5:1 (T/DC) for 3 days in the complete RPMI-1640 medium. Meanwhile, B16-F10 cells were seeded in a 96-well plate at a density of 2000 cells per well. Then the cocultured cells (T/DC) were collected and added to the B16-F10 cells at a ratio of 50:1 for 48-h incubation. Subsequently, the non-adherent T/DC cells were washed away and the viability of the adherent B16-F10 cells was measured according a standard MTT assay.

2.14. In vivo antigen presentation assay

At 24-h post subcutaneous immunization, the mice were killed and the inguinal lymph nodes and spleen were dissected to prepare the cell suspension by extruding through a 70-μm cell strainer (Falcon, BD, USA) using a syringe plunger. The cell suspension was then stained with anti-CD11c-FITC, anti-MHCI-FITC, and anti-MHCII-PE. The matured antigen-presenting cells were stained with anti-CD86-PE and measured by flow cytometry.

2.15. In vivo antitumor immunization

To determine the therapeutic efficacy of the vaccines, the BALB/c mice were subcutaneously injected with 0.1 mL of cell suspension containing 4×10^5 CT26 cells in the back close to the right shoulder. Five days after tumor inoculation, the hair on the back skin was shaved (an area of 3 cm^2). A microneedle array (Nanomed Skincare, Cupertino, USA) was applied to the naked skin and maintained in place for 2 min. After removal of the microneedle, the vaccines (recombinant proteins 50 μg, equal to 3.3 μg of antigenic peptide) were applied to the same region. After 3 h, the skin was washed with saline. The microneedle-assisted immunization was carried out for 3 times. There were five mice per group. The tumor size was measured using a vernier caliper and calculated by Eq. (2). The body weight was also monitored.

$$\text{Volume} = L \times W^2/2 \tag{2}$$

At the experimental endpoint of transcutaneous vaccination, the spleen was collected from the immunized mice, and the T cells from the spleen of each group were isolated as above mentioned. The T cells were then co-stained with anti-CD3 alpha-PerCP, anti-CD4-FITC, and anti-CD8-PE antibodies, and the percentage of $CD8^+$ and $CD4^+$ cells among the total T cells was determined by flow cytometry. Meanwhile, the isolated T cells were cultured for 24 h at 37 °C, and then treated with various protein formulations for 24 h at 37 °C. The cytokine levels of TNF-α, IL-2, and IL-10 in the coculture medium were measured by using the ELISA kits according to the manufacturer's instructions.

At the experimental endpoint, the tumors and the organs were dissected. The tumor growth inhibition rate was calculated based

on the tumor weights. The level of IFN-γ, TNF-α, IL-2, and IL-10 in the tumor were measured using the ELISA Kits.

To further investigate the cancer vaccination efficacy, subcutaneous injection of 5 μg of the vaccines (1/10 dose of the topical application) was used. The mice bearing CT26 tumor on their back close to the right shoulder were treated *via* subcutaneous injection in the other side of the back (ten mice per group). The survival rate was recorded.

For the preventive treatment regimen, the same dosage of rLTL group (n = 5) was applied before tumor challenge on Days −9, −6, and −3. The CT26 cells (4×10^5 per mouse) were inoculated (s.c.) on Day 0. Tumor growth was measured using a vernier caliper and calculated by Eq. (2).

2.16. The immunotherapy of rLTT

The rLTT vaccine was evaluated in the melanoma mouse model. The C57BL/6 mice were subcutaneously injected with 0.1 mL of cell suspension containing 3×10^5 B16-F10 cells on the back close to the right shoulder. The dose and immunization regimen were as described as above. After the therapy of transcutaneous vaccination, the $CD8^+$ T cells and $CD4^+$ T cells in spleen were also detected by flow cytometry. The intratumoral cytokine levels of TNF-α, IL-2 and TGF-β were determined by ELISA.

2.17. Immunofluorescence and immunohistochemistry assay

The dissected tumors at the experimental endpoint were mounted in the embedding compound for cryosection (CM190, Leica, Germany). The tumor slices were fixed with 4% paraformaldehyde for 15 min, and then incubated overnight at 4 °C with anti-legumain, anti-CD206, anti-Foxp3, anti-CD8α, anti-STING, or anti-IRF3 antibodies, respectively, and then with Alexa Fluor® 488-conjugated secondary antibody or 647-conjugated secondary antibody for 1 h at room temperature, and subsequently incubated with DAPI. The fluorescent images were obtained by laser scanning confocal microscopy (TCS-SP8, Leica, Germany).

The dissected tumors tissues were fixed with 4% paraformaldehyde and the paraffin section was processed for immunohistochemical examination of legumain and CD206 with a standard protocol.

2.18. Western blotting assay

The CT26 tumors dissected at the experimental endpoint were used to examine the expression of legumain, mannose receptor (CD206), TNF-α, and TGF-β using a standard Western blotting protocol.

2.19. Statistical analysis

Statistical analysis was performed by *t*-test and one-way ANOVA. Each experiment was performed in triplicate, and the data are represented as means ± standard deviation (S.D, $n = 3$, unless stated otherwise). Statistically significant differences were defined as $^{****}P < 0.0001$, $^{***}P < 0.001$, $^{**}P < 0.01$, $^{*}P < 0.05$, n.s, not significant.

3. Results

3.1. Preparation, cellular uptake and biocompatibility of recombinant protein vaccines

The plasmids pMXB10-TCS-leg and pMXB10-LTL were constructed to express TCS-lgmn$_{108-120}$ (rTCS-leg) and LMWP-TCS-lgmn$_{108-120}$ (rLTL) fusion proteins, respectively, using the IMPACT (intein-mediated purification with affinity chitin-binding tag) system (Fig. 1A and Supporting Information Fig. S1). The purified rTCS or rTCS-leg or rLTL were characterized by SDS-PAGE electrophoresis, size exclusion chromatography, and matrix-assisted laser desorption/ionization time-of-flight mass spectrometry (MALDI-TOF-MS, Fig. 1B−D).

The rLTL displayed a much higher uptake efficiency in DC2.4 dendritic cells (DC) than rTCS and rTCS-leg (Fig. 1E and F), due to the LMWP-enhanced intracellular delivery. CPP has been considered as a potent delivery tool but with non-specific nature in the blood stream delivery[20]. The cutaneous administration takes advantage of the penetration capacity of CPP, while avoiding the off-target to the normal organs as often seen in the i.v. injection, and thereby, CPP has been actively explored for cutaneous delivery[21].

The recombinant vaccines were not cytotoxic to DC at a dose up to 1 μmol/L (Fig. 1G), and thus could be safely applied as DC vaccine.

3.2. Antigen-presenting effect

The co-stimulatory factors of CD80 and CD86, serving as the indicators of DC maturation, are necessary to induce a potent tumor-specific cytotoxic T lymphocytes (CTL) response. Both CD80 and CD86 in the bone-marrow-derived dendritic cells (BMDCs) were significantly upregulated by the rLTL treatment compared to the control groups (Fig. 2A), as potent as the positive group of lipopolysaccharide (LPS).

Antigen presentation is mediated by major histocompatibility complex (MHC) molecules on the antigen-presenting cells (APCs) that display antigenic peptide fragments to the effector T cells. The BMDCs treated with rLTL showed an increased level of the MHC molecules (especially MHC class II, Fig. 2B). Moreover, the interferon-γ (IFN-γ) secretion from the $CD8^+$ T cells primed with the rLTL-treated BMDCs was significantly higher than other groups (Fig. 2C), indicating the effective activation of $CD8^+$ T cells.

The antigenic legumain peptide is a short sequence (13 amino acids). Typically, due to the small size, peptide antigens are not sufficient to elicit robust immune response. The immunogenicity of peptide antigens could be enhanced by conjugation with a carrier. In order to fully verify the adjuvant function of TCS, a control of LMWP-BSA-leg, in which BSA with non-adjuvant effect substituted TCS, was prepared. It was tested and the results showed LMWP-BSA-leg showed a minor effect on DC maturation, with an efficacy much lower than rLTL (Supporting Information Fig. S2).

There was a significantly different efficacy between rTCS-leg and TCS/leg. It can be explained as follows. First, the binding to MHC molecules occurs intracellularly, and thereby, the peptide epitopes must be delivered through the cell membrane and transported to the endoplasmic reticulum to the newly synthesized MHC molecules. Second, the immunogenicity of leg-peptide was enhanced by conjugation with the adjuvant TCS. Third, TCS can

bind with specific receptors on the cell membrane and enhance cellular uptake[22], and the fusion rTCS-leg could yield a higher cellular uptake than the leg-peptide in a mixture of TCS/leg.

3.3. *Antitumor immunotherapy studies*

The treatment efficacy of the “all-in-one” rLTL vaccine was examined in a CT26 colon tumor-bearing murine model (BALB/c mice) using microneedle-assisted transcutaneous vaccination. The rLTL vaccine exhibited the highest efficacy against tumor growth (82%), while the rTCS-leg group without LMWP had a tumor inhibition rate of 66%, and the mixture rTCS/leg was 48% and the antigenic peptide alone was merely 8% (Fig. 3A–C).

T cell-based cellular immunity is the key mechanism responsible for cancer therapeutic vaccination and the activation of effector $CD8^+$ T cells is a prerequisite for eliminating the target

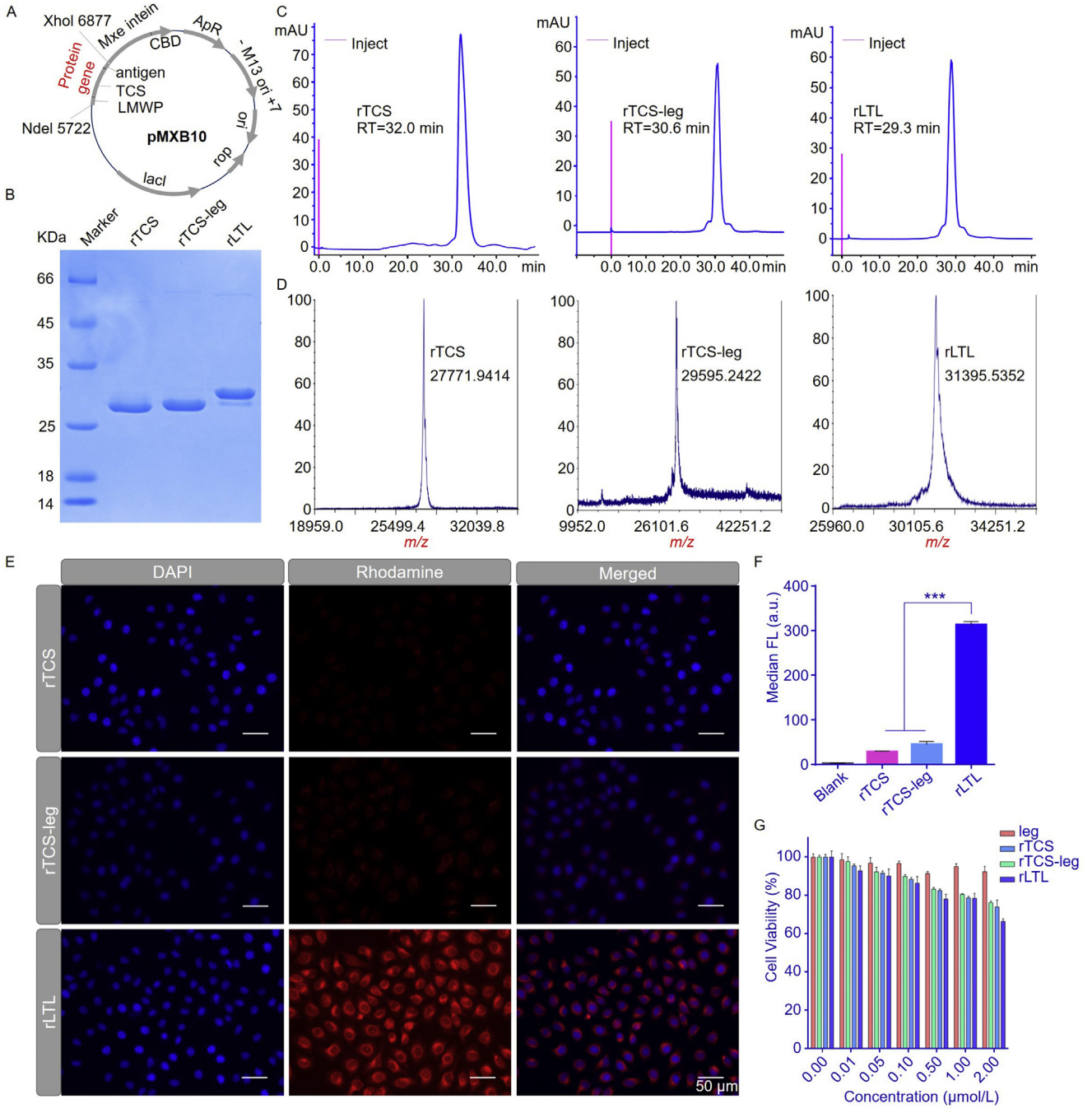

Figure 1 Characterization of the rLTL vaccine. (A) Plasmid encoding rLTL. (B) The SDS-PAGE electrophoresis. (C) Purity analysis of rTCS, rTCS-leg, and rLTL by size exclusion chromatography; retention time is related to the protein size. (D) MALDI-TOF-MS analysis. (E) Fluorescence images of the uptake of the fusion proteins in DC (scale bar, 50 μm). (F) The uptake efficiency of the protein vaccines in DC. (G) The fusion proteins showed minor cytotoxicity on DC at the tested dose ranges. Data are presented as mean ± SD ($n = 3$). ***$P < 0.001$.

cells. The amount of $CD8^+$ T cells in the spleen from the mice after treatment were measured to be 9.2% for rLTL, compared to 6.8% for the leg-peptide without TCS adjuvant, and the percentage of $CD4^+$ T cells was 18.8% for rLTL, and 15.4% for the leg-peptide (Fig. 3D). It indicated that the rLTL efficiently induced a T cell-mediated immunity. Furthermore, the cytokine analysis in the dissected tumors showed the significantly higher secretion of antitumor IFN-γ, tumor necrosis factor-α (TNF-α), and interleukin-2 (IL-2) induced by the rLTL treatment than other immunization (Fig. 3E). The antitumor $CD8^+$ T cells and M1 macrophages are characterized by the upregulated IFN-γ and TNF-α that are cytotoxic to the cancer cells. IL-2 plays a key role in driving the proliferation and activation of T and natural killer (NK) cells that possess cytolytic activity[23]. IL-10 is a major mediator for immune tolerance[24], which was seen a decrease after rLTL treatment (Fig. 3E).

To verify the antigen-specific cellular immunity responses, the isolated T cells from the spleens of the immunized mice were primed with the vaccines again, and resulted in the upregulated TNF-α and IL-2 levels but a reduction of IL-10 (Supporting Information Fig. S3).

TAM highly expressed legumain, and thus was the major target of the legumain-based vaccines[13,14]. The rLTL treatment led to the significant TAM annihilation, as represented by the reduction of the TAM biomarkers—mannose receptors (CD206) and legumain (Figs. 3F and 4, Supporting Information Fig. S5). TGF-β mainly secreted from TAM is a driving factor in tumor progression and exerts systemic immune suppression and inhibits host immunosurveillance[25,26]. The rLTL treatment reduced the TGF-β expression (Fig. 3F), demonstrating the effective annihilation of TAM. By contrast, there was an increase in the protumor TNF-α production (Fig. 3F), indicating the enhanced efficacy of immunotherapy.

Regulatory T cells (Treg) are a subset of T cells that mediate immunosuppression in tumor microenvironment. Our results showed that Foxp3, a Treg biomarker, was downregulated after vaccination, and the rLTL treatment led to the lowest expression among all the groups (Fig. 4). Importantly, the $CD8^+$ T cells in the tumor were significantly increased by the rLTL treatment (Fig. 4), suggesting the alleviation of immunosuppression and the enhanced CTL effect.

The immunological milieu of the skin is an ideal site for cutaneous vaccine delivery because there are abundant epidermis DCs (*i.e.*, Langerhans cells), accounting for a network of immune cells that underlie 25% of the total surface area in human skin[27]. As a self-administration technology, microneedle-assisted transcutaneous immunization has the advantages of painless and easy handling and accessibility, and therefore, it is a useful method for caner vaccination[28].

Furthermore, we also investigated the anticancer effectiveness of a traditional administration route—subcutaneous vaccination at a 1/10 dose of topical vaccination. There was a lower dosage setting used in subcutaneous vaccination considering the higher delivery efficiency of subcutaneous injection. Fig. 3G shows the survival curve of the mice and the rLTL group with a significantly prolonged survival time. Overall, these results demonstrated the efficacy of the rLTL vaccine and indicated such an "all-in-one" vaccine was promising for cancer immunotherapy.

Interestingly, in a tumor challenge study following vaccination, the mice that were pretreated with rLTL showed a slower tumor

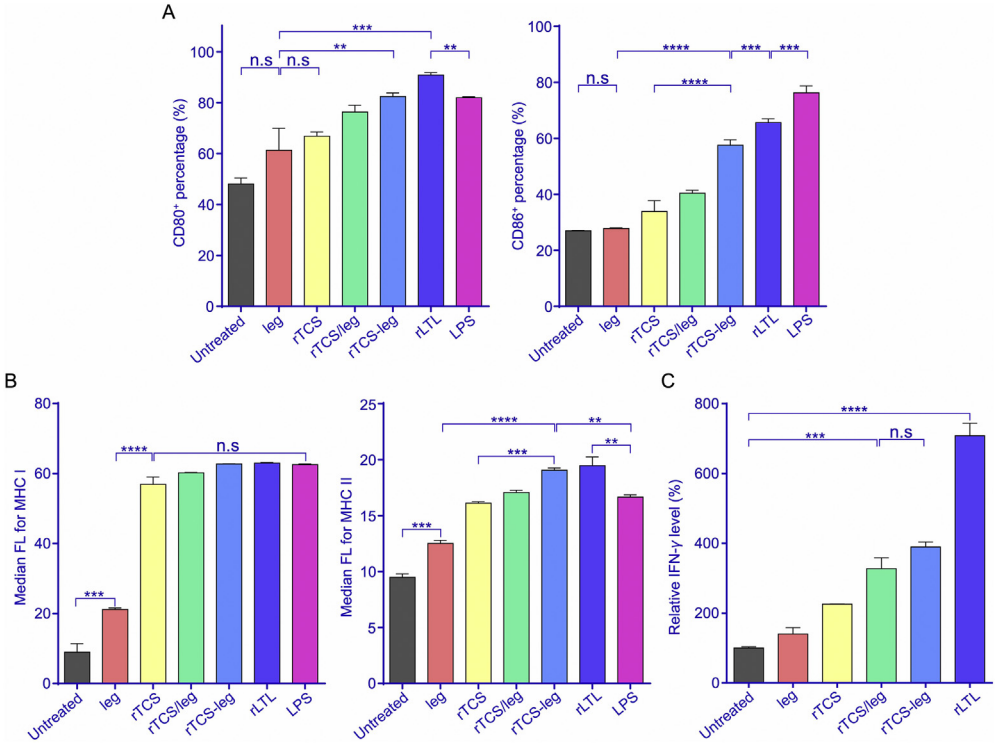

Figure 2 Antigen-presenting ability of rLTL vaccine. (A) The increased expression of CD80 and CD86 in DC induced by the vaccines. (B) Upregulation of MHC I & II molecules on BMDCs induced by the fusion proteins. (C) Increased IFN-γ secretion by $CD8^+$ T cells after primed by the BMDCs challenged with various protein vaccines. Data are presented as mean ± SD ($n = 3$). $^{****}P < 0.0001$, $^{***}P < 0.001$, $^{**}P < 0.01$, n.s, not significant.

development compared to the control group (Supporting Information Fig. S4). It suggested that TAM could also play an important role in the transplanted tumor formation and the preventive TAM annihilation retard the formation of tumor.

3.4. *TCS-TRP2 vaccination for immunotherapy*

To further demonstrate the universality of this TCS-adjuvant vaccination strategy, we used a tyrosinase-related protein-2 (TRP2) peptide as another model antigen and developed a cell-penetrating LMWP-TCS-TRP2 fusion protein vaccine (termed rLTT). TRP2 is a highly expressed by melanoma cells and can be recognized by the melanoma-specific CTL, and the TRP2 sequence (SVYDFFVWL) has been used as a promising cancer antigen[29,30].

The *in vitro* results showed an increased amount of matured DC and an enhanced level of MHC molecules induced by rLTT treatment (Supporting Information Fig. S6A and S6B), which revealed the potent antigen presentation ability. As a result, the rLTT-primed BMDCs efficiently elicited the antitumor IFN-γ secretion from the $CD8^+$ T cells (Supporting Information Fig. S6C), suggesting the activation of the effector $CD8^+$ T cells. Importantly, the effector T cell-mediated antigen-specific cytotoxicity was observed in the melanoma B16-F10 cells that overexpressed the antigen TRP2. The T cells isolated from the spleen primed by the rLTT-treated BMDCs were able to efficiently kill the B16-F10 cell (Supporting Information Fig. S6D).

For *in vivo* study, microneedle-assisted transcutaneous vaccination was carried out in the B16-F10 melanoma model (C57BL/6 mice). The tumor inhibition rate in each group was 18% (TRP2), 39.5% (rTCS), 52.7% (rTCS/TRP2), 60.6% (rTCS-TRP2), or 68.1% (rLTT), respectively (Fig. 5A–C). Due to the highly aggressive malignancy, no mice in the PBS control group survived longer than 16 days, and by contrast, the median survival of rLTT groups was 26 days (Fig. 5D). The amount of $CD4^+$ and $CD8^+$ T cells in the spleen and the intratumoral levels of the protumor

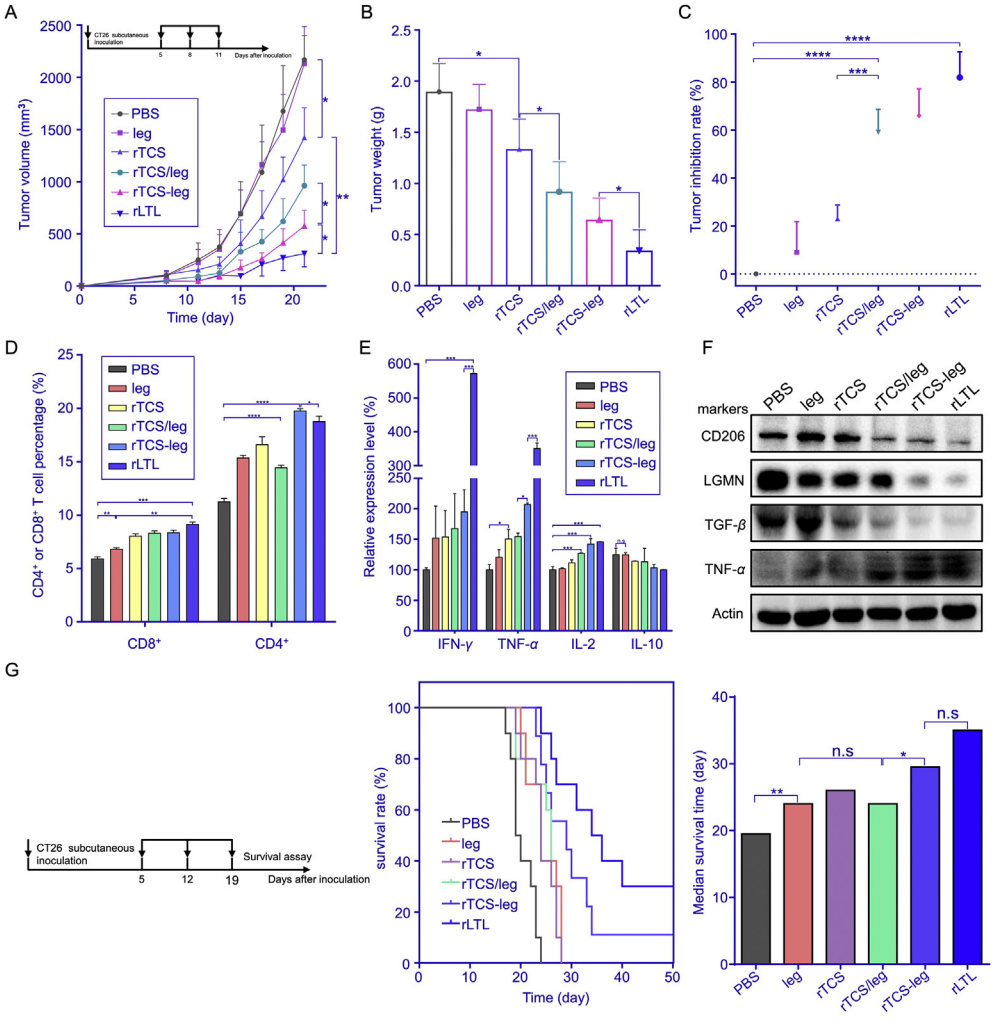

Figure 3 The immunotherapy of rLTL. (A) The treatment efficacy of microneedle-assisted vaccination in the CT26 tumor-bearing mice ($n = 5$). (B) Tumor weight at the treatment endpoint. (C) Inhibition rate of tumor growth. (D) Percentage of $CD8^+$ and $CD4^+$ T cells in the spleens of the mice after treatment. (E) The antitumor (IFN-γ, TNF-α, IL-2) and the protumor (IL-10) cytokine levels in the tumors after treatment. (F) Western blotting assay of the TAM-associated markers in the tumors. (G) Survival curve and median survival time of the mice receiving subcutaneous injection of the vaccines ($n = 10$). Data are presented as mean ± SD ($n = 3$). $^{****}P < 0.0001$, $^{***}P < 0.001$, $^{**}P < 0.01$, $^{*}P < 0.05$, n.s, not significant.

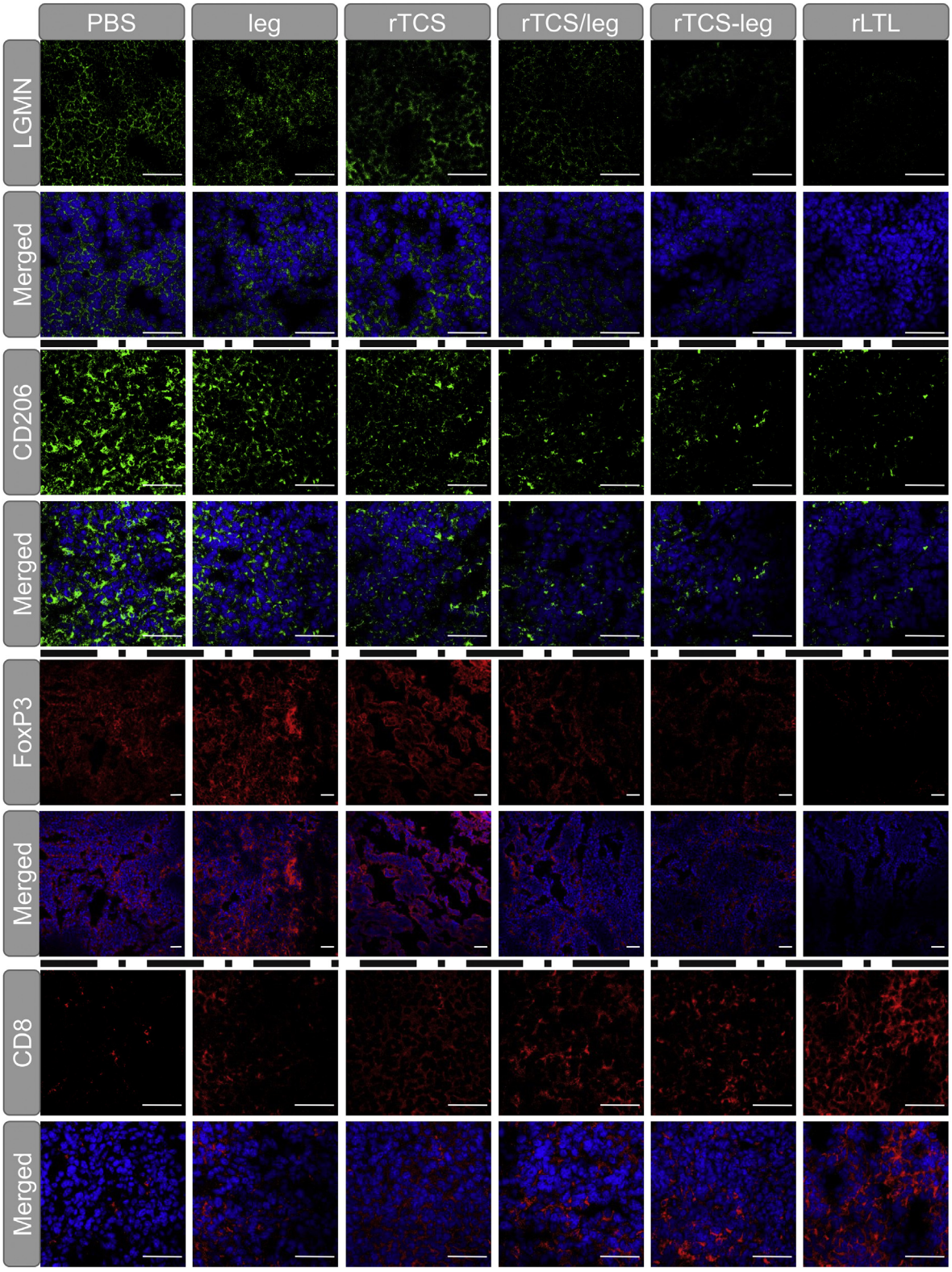

Figure 4 Immunofluorescence staining of the TAM biomarkers of legumain and CD206, as well as the FoxP3^{+} Treg and CD8^{+} T cells in the tumors after treatment. Scale bar, 50 μm.

cytokines (*e.g.*, TNF-α, IL-2, and IL-10) were also remarkably increased by rLTT treatment (Fig. 5E and F). These results indicated the successful induction of CTL-mediated antitumor immunity.

The tumor immune microenvironment was also examined after immunization. The expression of TAM-associated markers CD206 and legumain in the tumor were diminished after rLTT vaccination (Fig. 5G and H), suggesting the reduction of TAM. Accordingly, the protumor TGF-β, primarily secreted from TAM, was reduced (Fig. 5H). Moreover, the Tregs were suppressed while $CD8^+$ T cells were increased in the tumor tissues (Fig. 5I). It demonstrated that rLTT vaccination remodeled the tumor microenvironment by activating the CTL immunity while reducing the immunosuppressive TAM and Treg.

3.5. *The DC activation pathway*

The matured DC in the lymph nodes and spleens was analyzed. It showed that the matured DC (marked by CD86) was significantly increased after vaccination in the colon tumor animal model, compared to the PBS control group (Fig. 6A and B). Stimulator of interferon genes (STING) pathway plays an essential role in antitumor vaccination[31]. It was found that both STING and its downstream factor interferon regulatory factor 3 (IRF3) were

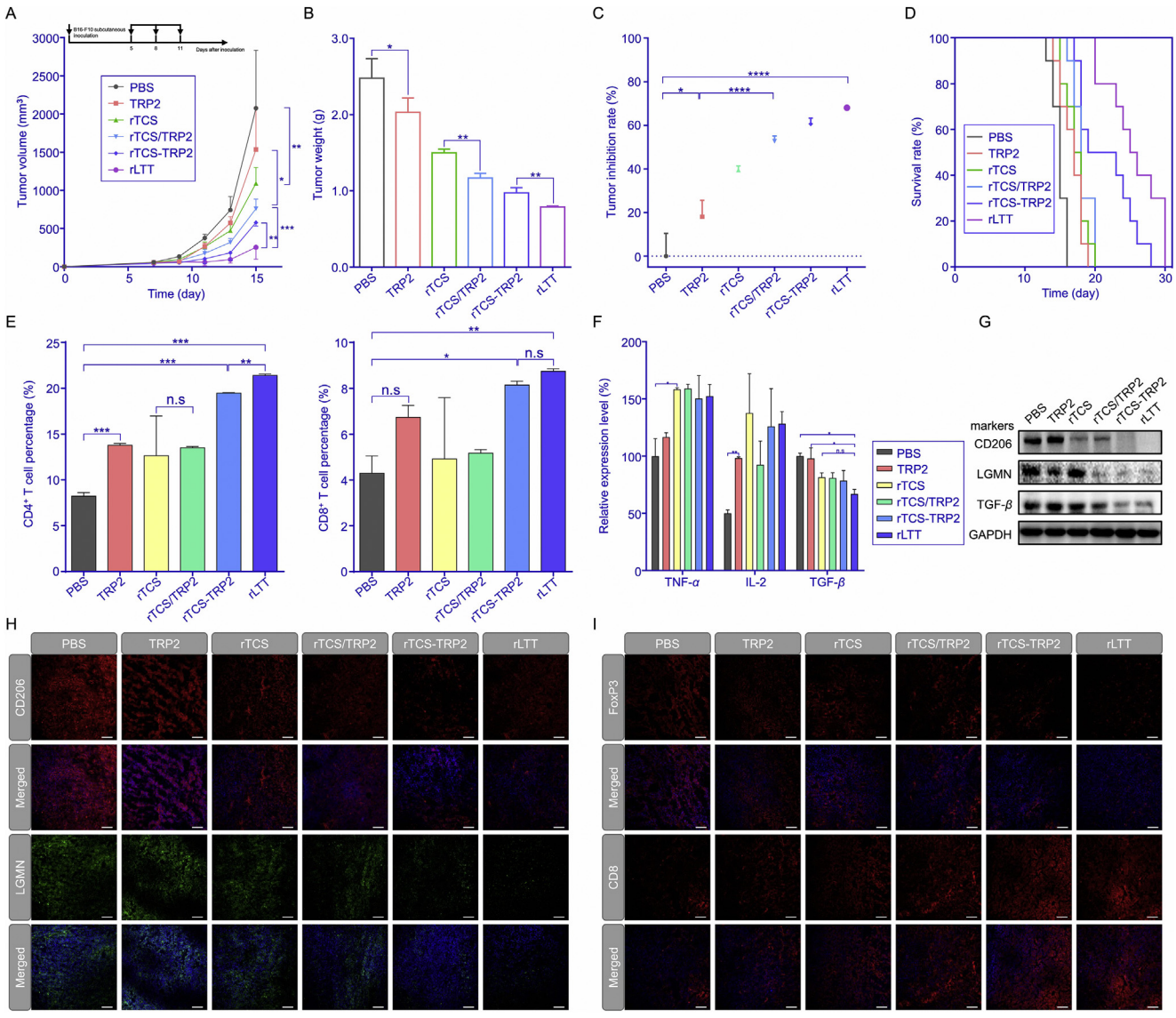

Figure 5 The rLTT vaccine for immunotherapy in the B16-F10 melanoma-bearing C57BL/6 mice. (A) Treatment efficacy of microneedle-assisted transcutaneous immunization ($n = 5$). (B) Tumor weight at the treatment endpoint. (C) Inhibition rate of tumor growth. (D) Survival curve and median survival time of the mice receiving transcutaneous vaccination ($n = 10$). (E) $CD8^+$ and $CD4^+$ T cells in the spleens of the mice after rLTT treatment were increased. (F) Cytokine levels in the tumors after microneedle-assisted immunization treatment. (G) Western blotting assay and (H) immunofluorescence staining of the TAM biomarkers (legumain and CD206) in the tumors after treatment. (I) Immunofluorescence staining of the $FoxP3^+$ Treg and $CD8^+$ T cells in the tumors after treatment. Scale bar, 100 μm. Data are presented as mean ± SD ($n = 3$). $^{****}P < 0.0001$, $^{***}P < 0.001$, $^{**}P < 0.01$, $^{*}P < 0.05$, n.s, not significant.

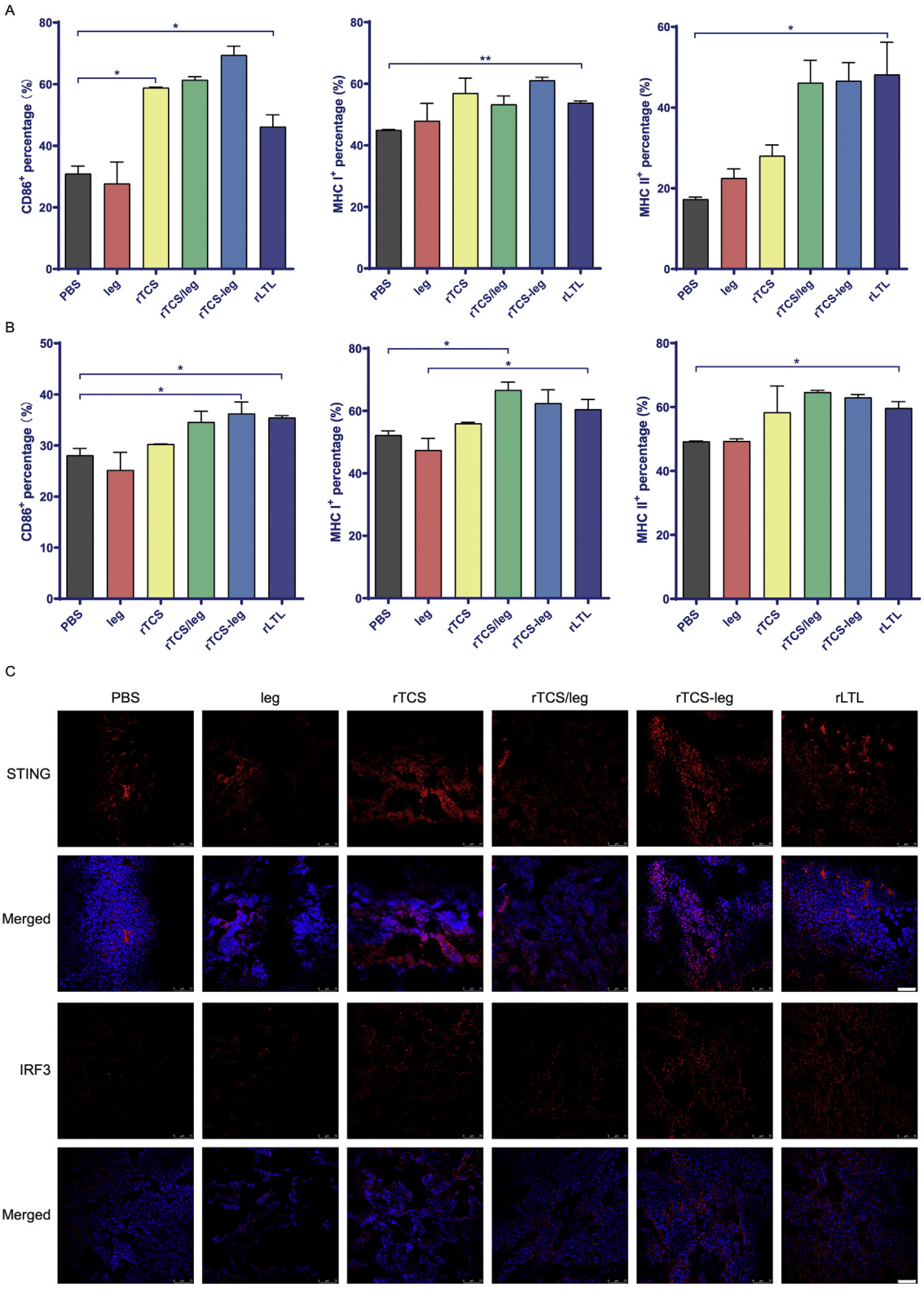

Figure 6 The immunostimulating mechanism study of rLTL in the CT26 colon tumor animal model. DC maturation measurement in the lymph node (A) and spleen (B) after treatment. (C) Immunofluorescent staining of STING and IRF3 in the tumors. Data are presented as mean ± SD ($n = 3$). $^{**}P < 0.01$, $^{*}P < 0.05$. Scale bar, 75 μm.

upregulated in the tumor after vaccination (Fig. 6C). The similar results were also observed in the melanoma animal model after vaccination (Supporting Information Fig. S7). It suggested the importance of the STING-IRF3 pathway in the TCS-stimulating immune responses. Yet, further investigation should be needed to illustrate the detailed molecular mechanisms.

3.6. *Preliminary evaluation of the biosafety*

The body weight loss was not found in all the groups and histopathological examination of the major organs did not show any observable toxicity in the vaccinated mice (Supporting Information Fig. S8), indicating the safety of recombinant TCS-based vaccination.

4. Discussion

In order to escape immune surveillance and survive, the cancer cells develop an elegant system to “educate” the immune cells and stroma cells around, thus forming the tumor immunosuppressive microenvironment[32]. For instance, an elevating amount of TAM and Tregs is closely related to the low response to tumor antigens[33]. A major barrier against successful translation of cancer vaccines is the insufficient efficacy to elicit robust DC-mediated immune effect. To develop an effective and safe immunostimulant is the essential part for cancer vaccination. TCS Injection is a clinically used gynecological drug in China for over three decades. In addition, its antitumor activity has been also well investigated. Our work demonstrated the new function of TCS as an immunostimulant for cancer vaccination.

It is interesting that TCS plays a dual role in immunomodulation—either immunosuppression[34] or immunostimulation[35]. Typically, TCS was found to elicit T helper 2 (Th2)-type immune responses in the naïve mice, with the elevating secretion of anti-inflammatory cytokines (*e.g.*, IL-10 and TGF-β)[36]. Conversely, in the tumor-bearing mice, TCS displayed the promotion of Th1-type immunity and the prolonged survival, but in the control group of naïve mice, it showed the decrease in the percentage of $CD8^+$ T cells and IFN-γ production[35]. It was also reported that TCS inhibited tumor growth more significantly in the immunocompetent mice than in the nude mice[5,35], suggesting the important role of T-cell immunity in TCS-based anticancer therapy.

Importantly, for the immunostimulating function, a low dose of TCS (*e.g.*, 0.25 mg/kg) can serve this purpose, compared to its ribosome inactivation-directed cytotoxic therapy dose of 2.5 mg/kg[4,5].

Recently, the use of low-dose chemo-drugs for facilitating immune activation has attracted great attention, of which the mechanisms involve DC maturation, the increased expression of auxiliary receptors in T cells, regulation of the cytokine network in immune microenvironment, and depletion of the immunosuppressive cells[28,37]. However, such application in cancer vaccination as an adjuvant still largely remains unknown. Our results clearly demonstrated the potency of TCS-assisted vaccination in various tumor models and vaccines. The immunoenhancing effect of TCS is associated with the action on promoting DC maturation and antigen presentation. STING is involved in the adjuvant function of TCS. Yet the molecular mechanisms still need to be further elucidated.

TCS was initially reported with immunosuppression effects that were associated with its anti-HIV activity. However, in the tumor-bearing model, TCS can enhance antitumor immune responses. For example, TCS increased the percentage of effector T cells, Th1 cytokine secretion, and elicited more memory T cells[35]. TCS increased Granzyme B penetration into tumor cells by upregulation of cation-independent mannose 6-phosphate receptor (CI-MPR), thus promoting cytotoxic T lymphocyte-mediated killing[38]. Moreover, TCS induced the cancer cells becoming more antigenic by promoting the synthesis of antigen peptides[39]. Therefore, it has been acknowledged that TCS has a bi-directional modulation on the immune systems, depending on the physico-pathologic conditions[35].

TAM is a promising therapeutic target for cancer therapy[40,41]. TAM as a vaccination target provides the unique advantages over cancer cells, in terms of the less mutation frequency and genetic variation.

It should be noted that a unique benefit of this reported method was its easy preparation and versatility. Based on the genetically-engineered TCS-based expression platform, the vaccines with various antigens can be designed and produced by simply incorporating a specific antigen-encoding DNA sequence into the plasmid system.

5. Conclusions

An efficient and safe adjuvant is an essential element for successful anticancer vaccination. The search for novel cancer immune stimuli has been active, but most of the reported ones lack druggability, with little prospect of clinical translation. In this work, a TCS-based fusion protein vaccine system was designed and the TCS-assisted cancer immunization strategy was developed. We firstly reported a novel cancer immunostimulatant for cancer vaccination and developed a versatile protein-engineering protocol for constructing a multifunctional “all-in-one” vaccine that were characterized by the easy fabrication and potent treatment efficacy. The translation of such an old drug into the new application would be cost- and time-saving and benefit from the well-documented safety of TCS from the decade-long clinical observation. The adaptability of this vaccine system is a unique advantage, of which any antigenic peptide or protein sequences can be incorporated into the genetically-engineered TCS-based expression platform, and it thus provides a feasible and useful method for cancer vaccination with potential clinical value.

Acknowledgments

We are thankful for the support of National Key Research and Development Program of China (2021YFE0103100, China), National Natural Science Foundation of China of China (81925035, 81673382, and 81521005, China), National Special Project for Significant New Drugs Development (2018ZX09711002-010-002, China), Shanghai SciTech Innovation Initiative (19431903100, 18430740800, China), and Shanghai Collaborative Innovation Group of Early Diagnosis and Precise Treatment of Hemangiomas and Vascular Malformations (SSMU-ZDCX20180701, China), Chinese Pharmaceutical Association-Yiling Pharm Joint Grants (CPAYLJ201901, China) for the support. We are also thankful for the National Center for Protein Science Shanghai, CAS, for MALDI-TOF MS assay. The original recombinant TCS plasmid was kindly provided by Prof. Pang-Chui Shaw, the Chinese University of Hong Kong.

Author contributions

Yongzhuo Huang and Qin Xu designed the research. Aihua Wu carried out the experiments and performed data analysis. Yingzhi Chen, Hairui Wang, Meng Zhang, Ya Chang, Pengfei Zhao, Yisi Tang, Zhuangzhi Zhu, and Yang Cao participated part of the experiments. Yongzhuo Huang and Aihua Wu wrote the manuscript. Yongzhuo Huang and Aihua Wu revised the manuscript. All of the authors have read and approved the final manuscript.

Conflicts of interest

The authors declare that there is no conflict of interest.

Appendix A. Supporting information

Supporting data to this article can be found online at https://doi.org/10.1016/j.apsb.2021.06.001.

References

1. Kumai T, Kobayashi H, Harabuchi Y, Celis E. Peptide vaccines in cancer-old concept revisited. *Curr Opin Immunol* 2017;**45**:1−7.
2. Temizoz B, Kuroda E, Ishii KJ. Vaccine adjuvants as potential cancer immunotherapeutics. *Int Immunol* 2016;**28**:329−38.
3. Shaw PC, Lee KM, Wong KB. Recent advances in trichosanthin, a ribosome-inactivating protein with multiple pharmacological properties. *Toxicon* 2005;**45**:683−9.
4. Chen YZ, Zhang M, Jin HY, Tang YS, Wang HY, Xu Q, et al. Intein-mediated site-specific synthesis of tumor-targeting protein delivery system: turning PEG dilemma into prodrug-like feature. *Biomaterials* 2017;**116**:57−68.
5. Chen YZ, Zhang M, Jin HY, Li DD, Xu F, Wu AH, et al. Glioma dual-targeting nanohybrid protein toxin constructed by intein-mediated site-specific ligation for multistage booster delivery. *Theranostics* 2017;**7**:3489−503.
6. Chen YZ, Zhang M, Jin HY, Tang YS, Wu AH, Xu Q, et al. Prodrug-like, PEGylated protein toxin trichosanthin for reversal of chemoresistance. *Mol Pharm* 2017;**14**:1429−38.
7. Reisfeld RA. The tumor microenvironment: a target for combination therapy of breast cancer. *Crit Rev Oncog* 2013;**18**:115−33.
8. Luo YP, Zhou H, Krueger J, Kaplan C, Lee SH, Dolman C, et al. Targeting tumor-associated macrophages as a novel strategy against breast cancer. *J Clin Invest* 2006;**116**:2132.
9. Dall E, Brandstetter H. Structure and function of legumain in health and disease. *Biochimie* 2016;**122**:126−50.
10. Jiang YF, Lu JY, Wang YP, Zeng F, Wang HY, Peng HG, et al. Molecular-dynamics-simulation-driven design of a protease-responsive probe for in-vivo tumor imaging. *Adv Mater* 2014;**26**:8174−8.
11. Guo PT, Zhu Z, Sun Z, Wang ZN, Zheng XY, Xu HM. Expression of legumain correlates with prognosis and metastasis in gastric carcinoma. *PLoS One* 2013;**8**:e73090.
12. Haugen MH, Boye K, Nesland JM, Pettersen SJ, Egeland EV, Tamhane T, et al. High expression of the cysteine proteinase legumain in colorectal cancer—implications for therapeutic targeting. *Eur J Cancer* 2015;**51**:9−17.
13. Luo YP, Zhou H, Krueger J, Kaplan C, Lee SH, Dolman C, et al. Targeting tumor-associated macrophages as a novel strategy against breast cancer. *J Clin Invest* 2006;**116**:2132−41.
14. Lewen S, Zhou H, Hu HD, Cheng T, Markowitz D, Reisfeld RA, et al. A Legumain-based minigene vaccine targets the tumor stroma and suppresses breast cancer growth and angiogenesis. *Cancer Immunol Immunother* 2008;**57**:507−15.
15. Smahel M, Duskova M, Polakova I, Musil J. Enhancement of DNA vaccine potency against legumain. *J Immunother* 2014;**37**:293−303.
16. Lee LM, Chang LC, Wrobleski S, Wakefield TW, Yang VC. Low molecular weight protamine as nontoxic heparin/low molecular weight heparin antidote (III): preliminary *in vivo* evaluation of efficacy and toxicity using a canine model. *AAPS PharmSci* 2001;**3**:E19.
17. Huang Y, Park YS, Moon C, David AE, Chung HS, Yang VC. Synthetic skin-permeable proteins enabling needleless immunization. *Angew Chem Int Ed* 2010;**49**:2724−7.
18. Yang YX, Jiang YF, Wang Z, Liu JH, Yan L, Ye JX, et al. Skin-permeable quaternary nanoparticles with layer-by-layer structure enabling improved gene delivery. *J Mater Chem* 2012;**22**:10029−34.
19. Choi JK, Jang JH, Jang WH, Kim J, Bae IH, Bae J, et al. The effect of epidermal growth factor (EGF) conjugated with low-molecular-weight protamine (LMWP) on wound healing of the skin. *Biomaterials* 2012;**33**:8579−90.
20. Huang Y, Jiang Y, Wang H, Wang J, Shin MC, Byun Y, et al. Curb challenges of the "Trojan Horse" approach: smart strategies in achieving effective yet safe cell-penetrating peptide-based drug delivery. *Adv Drug Deliv Rev* 2013;**65**:1299−315.
21. Tan J, Cheong H, Park YS, Kim H, Zhang M, Moon C, et al. Cell-penetrating peptide-mediated topical delivery of biomacromolecular drugs. *Curr Pharmaceut Biotechnol* 2014;**15**:231−9.
22. Jiao YZ, Liu WY. Low-density lipoprotein receptor-related protein 1 is an essential receptor for trichosanthin in 2 choriocarcinoma cell lines. *Biochem Biophys Res Commun* 2010;**391**:1579−84.
23. Sim GC, Radvanyi L. The IL-2 cytokine family in cancer immunotherapy. *Cytokine Growth Factor Rev* 2014;**25**:377−90.
24. Moore KW, de Waal Malefyt R, Coffman RL, O'Garra A. Interleukin-10 and the interleukin-10 receptor. *Annu Rev Immunol* 2001;**19**:683−765.
25. Yang L, Pang Y, Moses HL. TGF-beta and immune cells: an important regulatory axis in the tumor microenvironment and progression. *Trends Immunol* 2010;**31**:220−7.
26. Shevach EM. Role of TGF-β in the induction of Foxp3 expression and T regulatory cell function. *J Clin Immunol* 2008;**28**:640−6.
27. Glenn GM, Taylor DN, Li X, Frankel S, Montemarano A, Alving CR. Transcutaneous immunization: a human vaccine delivery strategy using a patch. *Nat Med* 2000;**6**:1403−6.
28. Xu JJ, Xu BH, Tao J, Yang YX, Hu Y, Huang YZ. Microneedle-assisted, DC-targeted codelivery of pTRP-2 and adjuvant of paclitaxel for transcutaneous immunotherapy. *Small* 2017;**13**:1700666.
29. Irvine AS, Trinder PK, Laughton DL, Ketteringham H, Mcdermott RH, Reid SC, et al. Efficient nonviral transfection of dendritic cells and their use for *in vivo* immunization. *Nat Biotechnol* 2000;**18**:1273.
30. Even MP, Bobbala S, Gibson B, Hook S, Winter G, Engert J. Twin-screw extruded lipid implants containing TRP2 peptide for tumour therapy. *Eur J Pharm Biopharm* 2017;**114**:79−87.
31. Luo M, Wang H, Wang ZH, Cai HC, Lu ZG, Li Y, et al. A STING-activating nanovaccine for cancer immunotherapy. *Nat Nanotechnol* 2017;**12**:648−54.
32. Zhu Y, Yu X, Thamphiwatana SD, Zheng Y, Pang Z. Nanomedicines modulating tumor immunosuppressive cells to enhance cancer immunotherapy. *Acta Pharm Sin B* 2020;**10**:2054−74.
33. Ghirelli C, Hagemann T. Targeting immunosuppression for cancer therapy. *J Clin Invest* 2013;**123**:2355−7.
34. Zhou XR, Yang NY, Lu LM, Ding Q, Jiao ZJ, Zhou Y, et al. Up-regulation of IL-10 expression in dendritic cells is involved in trichosanthin-induced immunosuppression. *Immunol Lett* 2007;**110**:74−81.
35. Cai YC, Xiong SD, Zheng YJ, Luo FF, Jiang P, Chu YW. Trichosanthin enhances anti-tumor immune response in a murine Lewis lung cancer model by boosting the interaction between TSLC1 and CRTAM. *Cell Mol Immunol* 2011;**8**:359−67.
36. Zhao SY, Wang YY, Wei HM. Trichosanthin induced Th2 polarization status. *Cell Mol Immunol* 2006;**3**:297−301.
37. Zheng YW, Dou Y, Duan LL, Cong CS, Gao AQ, Lai QH, et al. Using chemo-drugs or irradiation to break immune tolerance and facilitate immunotherapy in solid cancer. *Cell Immunol* 2015;**294**:54−9.

38. Li C, Zeng M, Chi H, Shen J, Ng TB, Jin G, et al. Trichosanthin increases Granzyme B penetration into tumor cells by upregulation of CI-MPR on the cell surface. *Oncotarget* 2017;**8**:26460−70.
39. Zhao JG, Huang CX, Yang GG, Jin JF, Kang YP, Xia DJ, et al. Preparation of anticolon carcinoma vaccine with rich chaperone peptides and study on its anticancer efficacy. *Chin J Gastrointest Surg* 2009;**12**:290−3.
40. Yang Q, Guo N, Zhou Y, Chen J, Wei Q, Han M. The role of tumor-associated macrophages (TAMs) in tumor progression and relevant advance in targeted therapy. *Acta Pharm Sin B* 2020;**10**:2156−70.
41. Tang X, Sui D, Liu M, Zhang H, Liu M, Wang S, et al. Targeted delivery of zoledronic acid through the sialic acid–Siglec axis for killing and reversal of M2 phenotypic tumor-associated macrophages—a promising cancer immunotherapy. *Int J Pharm* 2020;**590**:119929.